Rapid Communication in Photoscience(2015), vol. 4, no. 2, pp. 29-30
http://dx.doi.org/10.5857/RCP.2015.4.2.29 **ISSN 2288-4564(Online)**

Review

Emergence and Evolution of Organometal Halide Perovskite Solar Cell

Nam-Gyu Park*

School of Chemical Engineering, Sungkyunkwan University, Suwon 440-7462, Korea

ABSTRACT: Since the first report on long-term durable perovskite solar cell in 2012, a surge of interest in perovskite solar cell has been received due to its superb photovoltaic performance exceeding 20%. $MAPbI_3$ (MA = CH_3NH_3) perovskite film is able to be prepared simply by solution processes of either sequential two-step or single step procedure. Since $MAPbI_3$ shows balanced charge transport property with micrometer scale charge diffusion length, it can be applied to any kind of junction structures. Mostly studied structure is mesoscopic structure employing mesoporous oxide layer in perovskite film. Photovoltaic performance is primarily influenced by the quality of perovskite film but interfaces are equally important. In this mini review, emergence and evolution of perovskite solar cell are described.

Perovskite solar cell based on methylammonium lead halide, $MAPbX_3$ (MA = CH_3NH_3, X = Br, I) was first reported by Miyasaka group in 2009 using dye-sensitized solar cell structure [1]. A power conversion efficiency (PCE) of about 3-4% was demonstrated. An improved PCE of 6.5% was reported by Park group in 2011 [2]. Spin coating of the polar aprotic solvent such as *N*,*N*-dimethylformamide (DMF) or gamma-butyrolactone (GBL) solution containing MAI and PbI_2 on nanocrystalline TiO_2 film led to semi-spherical dot morphology of $MAPbI_3$. However, perovskite dots sitting on TiO_2 surface tends to be readily dissolved in polar solvent in electrolyte. Such instability hinders further development of perovskite solar cell. Park et al. eventually solved dissolution problem by employing solid state hole transport material (HTM), spiro-MeOTAD, which was reported in October 2012 [3]. Submicrometer-thick mesoporous TiO_2 film was decorated with perovskite dots and the pores were filled with spiro-MeOTAD, which demonstrated a PCE of 9.7%. It was found that PCE was improved as the TiO_2 film thickness decreased, which was mainly due to high absorption coefficient of more than 10^4 cm^{-1} [2, 3]. Transient absorption spectroscopic study showed effective charge separation occurred between perovskite and hole transport spiro-MeOTAD, which indicates that valance band of perovskite and HOMO level of spiro-MeOTAD is well matched for injection of holes from perovskite to HTM. In Figure 1, structure of $MAPbI_3$ and energy levels among TiO_2, $MAPbI_3$ and spiro-MeOTAD are schematically depicted, where methylammonium cation is located in cubo-octahedral site and Pb-I octahedra are corner shared.

Since oraganometal halide perovskite is ionic crystal, it can be prepared by solution process under mild condition. Since lattice energy of halide perovskite is lower than that of covalent oxides due to low Madelung constant [4], $MAPbI_3$ can be formed even at ambient temperature without heat treatment. $MAPbI_3$ is formed via either one-step or sequential two-step procedure. For one-step spin coating, polar aprotic solvent containing PbI_2 and MAI is used to form $MAPbI_3$. PbI_2 layer is first formed in two-step procedure, which is followed by spin-coating of MAI. This leads to $MAPbI_3$ according to eq 1.

***To whom correspondence should be addressed.**
E-mail: npark@skku.edu

$$PbI_2\ (s) + MAI\ (l) \rightarrow MAPbI_3\ (s) \qquad (1)$$

Morphology of one-step coated MAPbI3 is different from that of two-step one. Without any specific process involved in two methods, photovoltaic performance of perovskite solar cell prepared by one-step is found to be inferior to that of two-step method [5].

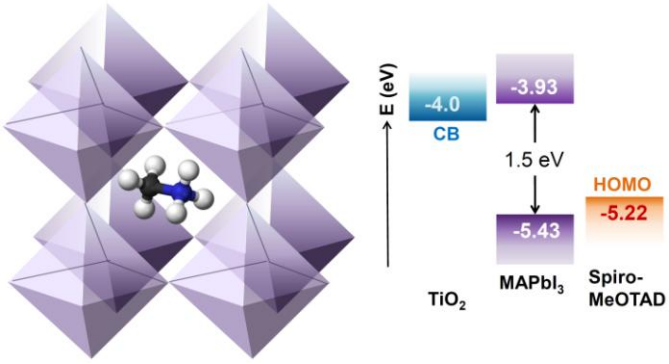

Figure 1. Local structure of $MAPbI_3$ perovskite showing lead-iodide octahedral and cubo-octahedral MA. Band positions of perovskite along with those for TiO_2 and spiro-MeOTAD.

However, one-step method is expected to be superior to two-step procedure if crystal growth is controlled. Regarding two-step procedure, it was found that crystal size was controlled by varying MAI concentration, where relatively large crystal formed from low concentration but small size formed from high concentration [6].

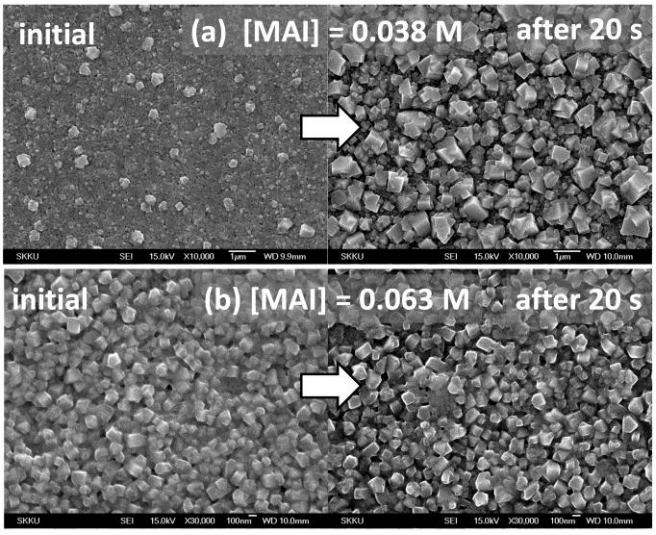

Figure 2. SEM images showing dependence of crystal growth on MAI concentration of (a) 0.038 M and (b) 0.063 M.

Figure 2 shows evolution of crystal growth with time. At low

concentration of 0.038 M, small seed crystals are sparsely formed initially, which grows bigger with time. On the other hands, seed crystals are closely packed initially at high concentration of 0.063 M without further growth with time. Photovoltaic performance was found to significantly depend on $MAPbI_3$ size. Large grain $MAPbI_3$ grown from low concentration showed higher photocurrent and fill factor than small one from high concentration. However, lower voltage was observed for large grain than for medium and small grains. Large crystal with gaps between crystals was found to be beneficial to light harvesting, resulting in high photocurrent. High fill factor could be related to ferroelectric property of $MAPbI_3$ [7]. Change in voltage with crystal size can be explained by difference in charge mobility and extraction ability. As can be seen in Figure 3, amount of the extracted charges increase with increasing size. However, 800 nm-size shows slower hole mobility than 200 nm- and 100 nm-size, which is responsible for lower voltage because of increased chance of recombination.

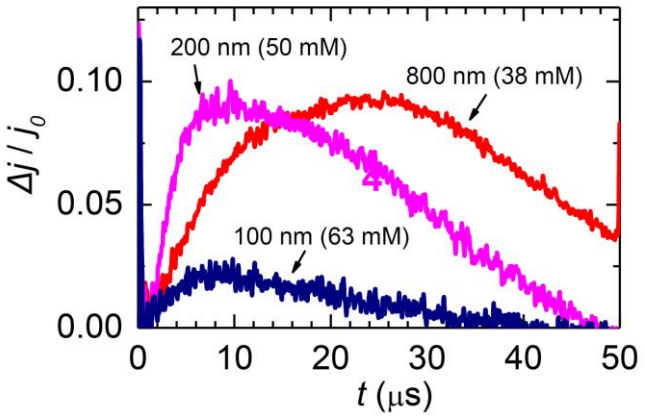

Figure 3. Photo-CELIV results for $MAPbI_3$ with size of 100 nm, 200 nm and 800 nm grown from SEM images showing dependence of crystal growth on MAI concentration of (a) 0.038 M and (b) 0.063 M.

Except for $MAPbI_3$, formamidinium (FA) cation can be stabilized in A-site of ABX_3 perovskite because of similar cationic size. Two-step deposited $FAPbI_3$ showing a PCE of 16% was found to be better in photostability than $MAPbI_3$ [8]. This might be related to phase transition issue. In the mesoscopic structure using mesoporous TiO_2 layer, it has been issued whether or not electrons generated in perovskite are injected to TiO_2. From the anatase and rutile TiO_2 layers and the nanohelix structure, electron injection was evident but injection happened in part [9,10]. As an oxide scaffold, 1-dimensional nanorods are expected to be good candidates because they provide suitable structure for better charge separation and transport as well. ZnO nanorod was applied to perovskite solar cell and confirmed to be good material for electron transport [11,12]. Solution processed and vacuum processed perovskites were reported to be 3-dimensional morphology. We recently prepared 1-dimensional $MAPbI_3$ by two-step solution process, where 1-dimensional growth of $MAPbI_3$ could be explained by liquid catalyst cluster model [13]. 1-D perovskite exhibited faster charge separation, higher conductivity, longer life time against radiative recombination than 3-D cuboid one.

In summary, organometal halide perovskite is very promising photovoltaic material owing to its superb opto-electronic property. In addition, facile fabrication process renders perovskite solar cell possible for low-cost mass production. Nevertheless, there are some critical issues to be solved such as moisture and thermal instability and lead toxicity. Progress in perovskite solar cell along with physic-chemical property of perovskite material is found from the review articles [14-16].

KEYWORDS: perovskite, solar cell, oagnometal halide, emergence

Received June 8, 2015; Accepted June 27, 2015

ACKNOWLEDGEMENT

This work was supported by the National Research Foundation of Korea (NRF) grants funded by the Ministry of Science, ICT & Future Planning (MSIP) of Korea under contracts No. NRF-2012M1A2A2671721, NRF-2012M3A7B4049986 (Nano Material Technology Development Program), NRF-2012M3A6A7054861 (Global Frontier R&D Program on Center for Multiscale Energy System).

REFERENCES AND NOTES

1. Kojima, A.; Teshima, K.; Shirai, Y.; Miyasaka, T. *J. Am. Chem. Soc*. **2009**, *131*, 6050-6051.
2. Im, J.-H.; Lee, C.-R.; Lee, J.-W.; Park, S.-W.; Park, N.-G. *Nanoscale* **2011**, *3*, 4088-4093.
3. Kim, H.-S.; Lee, C.-R.; Im, J.-H.; Lee, K.-B.; Moehl, T.; Marchioro, A.; Moon, S.-J.; Humphry-Baker, R.; Yum, J.-H.; Moser, J. E.; Grätzel, M.; Park, N.-G. *Sci. Rep*. **2012**, *2*, 591.
4. Jung, H. S.; Park, N.-G. *Small*, **2015**, 11, 10-25.
5. Im, J.-H.; Kim, H.-S.; Park, N.-G. *APL Materials*, **2015**, 2, 081510.
6. Im, J.-H.; Jang, I.-H.; Pellet, N.; Grätzel, M.; Park, N.-G. **2014**, *Nat. Nanotechnol.* 9, 927-932.
7. Kim, H.-S.; Kim, S. K.; Kim, B. J.; Shin, K.-S.; Gupta, M. K.; Jung, H. S.; Kim, S.-W.; Park, N.-G. *J. Phys. Chem. Lett*. **2015**, 6, 1729–1735.
8. Lee, J.-W.; Seol, D.-J.; Cho, A.-N.; Park, N.-G. *Adv. Mater***. 2014**, 26, 4991-4998.
9. Lee, J.-W.; Lee, T.-Y.; Yoo, P. J. Grätzel, M.; Mhaisalkar, S.; Park, N.-G. *J. Mater. Chem. A*, **2014**, 2, 9251-9259.
10. Lee, J.-W.; Lee, S. H.; Ko, H.-S.; Kwon, J.; Park, J. H.; Kang, S. M.; Ahn, N.; Choi, M.; Kim, J. K.; Park, N.-G. *J. Mater. Chem. A*, **2015**, 3, 9179-9186.
11. Son, D.-Y.; Im, J.-H.; Kim, H.-S.; Park, N.-G. *J. Phys. Chem. C*, **2014**, 118, 16567-16573.
12. Son, D.-Y.; Bae, K.-H.; Kim, H. S.; Park, N.-G. *J. Phys. Chem. C*, **2015**, 119, 10321–10328
13. Im, J.-H.; Luo, J.; Franckevičius, M.; Pellet, N.; Gao, P.; Moehl, T.; Zakeeruddin, S. M.; Nazeeruddin, M. K.; Grätzel, M.; Park, N.-G. *Nano Lett*., **2015**, 15, 2120-2126.
14. Park, N.-G. *J. Phys. Chem. Lett*., **2013,** 4, 2423-2429.
15. Kim, H.-S.; Kim, S. H.; Park, N.-G. *J. Phys. Chem. C*, **2014**, 118, 5615-5625.
16. Park, N.-G. *Mater. Today*, **2014**, 15, 65-72.